

UC Santa Barbara

UC Santa Barbara Previously Published Works

Title

Dimensionality effects on trap-assisted recombination: the Sommerfeld parameter

Permalink

<https://escholarship.org/uc/item/9ct5w9fn>

Journal

Journal of Physics Condensed Matter, 36(19)

ISSN

0953-8984

Authors

Turiansky, Mark E

Alkauskas, Audrius

Van de Walle, Chris G

Publication Date

2024-05-15

DOI

10.1088/1361-648x/ad2588

Peer reviewed

1 Dimensionality Effects on Trap-Assisted
2 Recombination: The Sommerfeld Parameter

3 Mark E. Turiansky¹, Audrius Alkauskas²‡, and Chris G.
4 Van de Walle¹

5 ¹ Materials Department, University of California, Santa Barbara, CA
6 93106-5050, U.S.A.

7 ² Center for Physical Sciences and Technology (FTMC), Vilnius LT-10257,
8 Lithuania

9 E-mail: mturiansky@ucsb.edu

10 **Abstract.** In the context of condensed matter physics, the Sommerfeld
11 parameter describes the enhancement or suppression of free-carrier charge density
12 in the vicinity of a charged center. The Sommerfeld parameter is known for
13 three-dimensional systems and is integral to the description of trap-assisted
14 recombination in solids. Here we derive the Sommerfeld parameter in one
15 and two dimensions and compare with the results in three dimensions. We
16 provide an approximate analytical expression for the Sommerfeld parameter in
17 two dimensions. Our results indicate that the effect of the Sommerfeld parameter
18 is to suppress trap-assisted recombination in decreased dimensionality.

19 Submitted to: *J. Phys.: Condens. Matter*

‡ Deceased.

20 1. Introduction

21 Charged defects and impurities play an important role in condensed matter systems,
 22 leading to a variety of physics including as centers of carrier recombination. In the
 23 presence of a charged center, the free-carrier wavefunction is perturbed, leading to an
 24 enhancement or suppression of the carrier charge density in the vicinity of the center.
 25 This perturbation has been thoroughly analyzed in the case of bulk material and is
 26 commonly quantified as the Sommerfeld parameter [1, 2, 3, 4, 5]. The Sommerfeld
 27 parameter also arises in fields other than condensed matter physics, for example, in
 28 the description of dark matter in high-energy astrophysics [6, 7, 8].

29 Understanding trap-assisted recombination at defects or impurities is of utmost
 30 importance for improving device performance. In optoelectronic devices such as light-
 31 emitting diodes or solar cells, the so-called Shockley-Read-Hall process allows carriers
 32 to recombine nonradiatively, transferring the excitation energy into lattice vibrations
 33 and reducing the emission efficiency. Point defects and impurities may also act as
 34 charge traps, capturing free carriers and degrading performance. First-principles
 35 formulations to evaluate nonradiative recombination rates exist [9, 10, 11, 12], and
 36 the calculated rates are scaled by the Sommerfeld parameter when a charged center
 37 is involved. For example, the nonradiative capture coefficient is given by $C = s(T)\tilde{C}$,
 38 where $s(T)$ is the temperature-dependent Sommerfeld parameter and \tilde{C} is the capture
 39 coefficient calculated in a neutral defect-containing supercell. This scaling is necessary
 40 because typical supercells used in first-principles calculations are insufficiently large to
 41 describe the long-ranged Coulomb potential of the charged center. The Sommerfeld
 42 parameter also plays a role in radiative capture [13] and trap-assisted Auger-Meitner
 43 recombination [14].

44 Many relevant device architectures involve lower-dimensional structures. For
 45 example, light-emitting diodes utilize quantum wells, in which carriers are confined
 46 and behave as if they are quasi-two-dimensional. Going further, semiconductor
 47 nanowires, in which confinement of carriers leads to quasi-one-dimensional behavior,
 48 are being explored for next-generation optoelectronic devices [15]. Semiconductor
 49 nanowires [16] and gate-defined quasi-one-dimensional wires derived from a two-
 50 dimensional electron gas [17] have been employed in the search for Majorana bound
 51 states. Devices are getting ever smaller, and quantum effects and dimensionality
 52 play a larger role. In addition, two-dimensional materials, such as hexagonal boron
 53 nitride, are being considered for electronic devices through the construction of van der
 54 Waals heterostructures [18]. Two-dimensional materials are also promising hosts for
 55 quantum defects [19, 20, 21], particularly for applications in quantum metrology [22].
 56 Quasi-one-dimensional materials, such as carbon nanotubes, are also being explored
 57 as hosts for quantum defects [23, 24]. Of course, lower-dimensional systems still exist
 58 in three dimensions; while the wavefunction in the confined directions is not constant,
 59 studying an idealized lower-dimensional system provides important insight into the
 60 effects of dimensionality since it allows focusing on the key long-range effects.

61 In this work, we assess the effect of dimensionality on trap-assisted recombination
 62 by studying the Sommerfeld parameter. We first review the derivation of the
 63 Sommerfeld parameter in three dimensions (3D) and then derive the Sommerfeld
 64 parameter in two (2D) and one (1D) dimensions, comparing to the case of 3D. We
 65 provide an approximate analytical expression for the temperature dependence in 2D
 66 and assess the accuracy of the utilized approximations in 2D and 3D. In 1D, an
 67 explicit formula cannot be obtained and instead direct numerical evaluation is used.

68 Overall we find that reduced dimensionality suppresses trap-assisted recombination
 69 through the Sommerfeld parameter. This result has important implications for device
 70 performance. We have implemented these developments in the latest version of
 71 the Nonrad code [25, 12], which is an open-source Python code that evaluates the
 72 nonradiative capture rate from first principles.

73 In Sec. 2, we formulate the problem of a charged center in an effective medium
 74 through the Wannier equation and derive the Sommerfeld parameter in different
 75 dimensions. We review the derivation of the Sommerfeld parameter in 3D in Sec. 2.1,
 76 and derive the Sommerfeld parameter in 2D in Sec. 2.2 and in 1D in Sec. 2.3. In
 77 Sec. 3, we discuss the results from our derivations, in particular assessing the effects
 78 of dimensionality and the numerical stability of the employed approximations. We
 79 comment on the implications of these results for devices and experiments in Sec. 4:
 80 Reduced recombination in lower dimensions will be favorable for device performance.
 81 Section 5 concludes the paper.

82 2. Derivation of the Sommerfeld Parameter

83 We seek to describe the perturbation of a carrier wavefunction in the presence of a
 84 Coulomb center. We will first focus on electrons and comment on the case of holes at
 85 the end of this section. We write down a single-particle Schrödinger equation for an
 86 electron in a periodic potential in the presence of a perturbation (in SI units),

$$87 \quad \left[-\frac{\hbar^2}{2m_e} \nabla^2 + V(\mathbf{r}) + U(\mathbf{r}) \right] \psi = E\psi, \quad (1)$$

88 where m_e is the free electron mass and $V(\mathbf{r})$ is the periodic potential that the
 89 electron experiences. U is the Coulomb center potential and is given by $U(\mathbf{r}) =$
 90 $(Z/4\pi\epsilon_r\epsilon_0)(e^2/|\mathbf{r}|)$. Z is the charge of the Coulomb center (in units of the elementary
 91 charge e), ϵ_0 is the vacuum permittivity, and ϵ_r is the static relative permittivity of
 92 the material.

93 The Coulomb center potential U constitutes a minor and slowly varying
 94 perturbation, and therefore the Bloch functions form a natural basis for expanding the
 95 eigenfunction ψ . Luttinger and Kohn [26] provided an ansatz for the wavefunction,
 96 thus providing the foundation of effective mass theory,

$$97 \quad \psi(\mathbf{r}) = \sqrt{\mathcal{N}_0\Omega_0} \phi(\mathbf{r}) u_{\mathbf{k}_0}(\mathbf{r}), \quad (2)$$

98 where $u_{\mathbf{k}_0}$ is the unperturbed Bloch function of the crystal at the band extremum
 99 located at wavevector \mathbf{k}_0 . \mathcal{N}_0 is the number of unit cells that the wavefunction extends
 100 over. Ω_0 is the volume of the unit cell in 3D; in 2D it is the area, and in 1D, the length
 101 of the unit cell. $\phi(\mathbf{r})$ is the envelope function, which we will solve for.

102 For an electron in an isotropic parabolic band, the energy $E \approx E_0 +$
 103 $\hbar^2|\mathbf{k} - \mathbf{k}_0|^2/2m^*$, where m^* is the band effective mass. Furthermore, we will assume
 104 that the band extremum occurs at the Γ point ($\mathbf{k}_0 = \mathbf{0}$) and that the extremum is
 105 non-degenerate. These assumptions do not affect the generality of our results, and we
 106 comment on their influence in Sec. 3. Under these assumptions, equation 1 may be
 107 reduced to the Wannier equation [27, 28, 29, 30, 2]

$$108 \quad \left[-\frac{\hbar^2}{2m^*} \nabla^2 + U(\mathbf{r}) \right] \phi(\mathbf{r}) = \varepsilon\phi(\mathbf{r}), \quad (3)$$

109 which may be solved for the envelope function ϕ . ε is the corresponding eigenenergy
 110 for the envelope function and is referenced to the band extremum E_0 .

111 In deriving the Sommerfeld parameter, we are most interested in the continuum
 112 solutions of equation 3, i.e. $\varepsilon = \hbar^2 k^2 / 2m^* > 0$. Therefore k will be a good quantum
 113 number for the envelope function. The envelope function also implicitly depends on Z ,
 114 which sets the Coulomb center potential. In the following sections, we will explicitly
 115 include the labels Z and k in the notation for the envelope function, $\phi_k^Z(\mathbf{r})$. An
 116 important limit to consider is the absence of the Coulomb center potential, where
 117 $Z = 0$. In this case, it must be true that

$$118 \quad \phi_k^0(r) = e^{ikr} / \sqrt{\mathcal{N}_0 \Omega_0}, \quad (4)$$

119 or in other words, the wavefunction in equation 2 should be equivalent to the
 120 unperturbed Bloch function of the crystal $u_{\mathbf{k}_0}$.

121 The above arguments can be generalized to the case when the carrier corresponds
 122 to a hole in the valence band by a judicious change of sign. What matters in the end
 123 is whether the Coulomb potential corresponds to an attractive or repulsive potential.
 124 In other words, one should regard Z not as the Coulomb center charge, but as the
 125 product of the Coulomb center charge and the charge of the carrier (both in units
 126 of the elementary charge e). With this definition, $Z > 0$ ($Z < 0$) corresponds to a
 127 repulsive (attractive) potential.

128 2.1. Three Dimensions

129 First we review the derivation in 3D, as it will provide guidance for the derivation in
 130 2D and 1D. In 3D, equation 3 is most readily solved in spherical coordinates. Standard
 131 separation of variables permits us to write

$$132 \quad \phi_k^Z(\mathbf{r}) = R_{kl}(r) Y_{lm}(\theta, \varphi), \quad (5)$$

133 where $R_{kl}(r)$ is a function of the radial variable r . $Y_{lm}(\theta, \varphi)$ are the spherical
 134 harmonics in the angular variables (θ, φ) and are indexed by l and m . Inserting
 135 equation 5 into equation 3 provides an equation to solve for the radial function,

$$136 \quad \left(\frac{\partial^2}{\partial r^2} + \frac{2}{r} \frac{\partial}{\partial r} - \frac{\gamma}{r} + k^2 - \frac{l(l+1)}{r^2} \right) R_{kl}(r) = 0 \quad (6)$$

137 where $\gamma = 2Z/a^*$ and $a^* = 4\pi\epsilon_r\epsilon_0\hbar^2/(m^*e^2)$ is the effective Bohr radius.

138 The solutions to equation 6 have the form [5, 31, 32, 33]

$$139 \quad R_{kl}(r) = C_{kl} e^{-ikr} r^l F(1+l-i\nu, 2l+2, 2ikr), \quad (7)$$

140 where $\nu = \gamma/2k = Z/a^*k$ and C_{kl} is a normalization coefficient to be determined. F
 141 is the regular confluent hypergeometric series given by

$$142 \quad F(\alpha, \beta, \xi) = 1 + \frac{\alpha}{\beta} \frac{\xi}{1!} + \frac{\alpha(\alpha+1)}{\beta(\beta+1)} \frac{\xi^2}{2!} + \dots \quad (8)$$

143 At large distances ($r \rightarrow \infty$), equation 7 becomes

$$144 \quad R_{kl}(r) = \frac{C_{kl}}{kr} \frac{\Gamma(2l+2)}{(2k)^l} \frac{e^{\pi\nu/2}}{|\Gamma(1+l+i\nu)|} \times \quad (9)$$

$$\cos\left(kr - \nu \log(2kr) - \frac{\pi}{2}(l+1) - \sigma_l\right),$$

144 where Γ is the Gamma function, and σ_l is the complex phase of the Gamma function,
 145 given by

$$146 \quad \sigma_l = \arg \Gamma(1+l+i\nu). \quad (10)$$

147 The wavefunctions of the continuous spectrum resemble spherical waves far from the
148 Coulomb center.

149 To determine the normalization coefficient C_{kl} , we apply the normalization
150 condition “in k scale” [31]:

$$151 \int_0^\infty dr r^2 R_{kl}(r) \int_{k-\Delta k}^{k+\Delta k} dk' R_{k'l}(r) = 1, \quad (11)$$

152 where Δk is a small interval. Applying the normalization condition to the asymptotic
153 form of the radial function (equation 9) we obtain

$$154 C_{kl} = \sqrt{\frac{2}{\pi}} \frac{k(2k)^l}{\Gamma(2l+2)} \sqrt{\frac{2\pi\nu}{e^{2\pi\nu}-1} \prod_{s=1}^l [s^2 + \nu^2]}. \quad (12)$$

155 The spherical harmonics were convenient to solve equation 3. However, to satisfy
156 equation 4 and derive the Sommerfeld parameter, it is more convenient to switch
157 our approach to that of a scattering problem. For this, we utilize the partial-wave
158 expansion [5],

$$\phi_k^Z(\mathbf{r}) = \frac{(2\pi)^{3/2}}{\sqrt{\mathcal{N}_0\Omega_0}} \frac{1}{4\pi k} \times \sum_{l=0}^{\infty} i^l (2l+1) e^{i\delta_l} P_l(\mathbf{k} \cdot \mathbf{r}/kr) R_{kl}(r), \quad (13)$$

159 where δ_l are the scattering phases and P_l are the Legendre polynomials. R_{kl} is
160 the radial wavefunction given in equation 7 with the normalization determined in
161 equation 12. However, we have adjusted the normalization of equation 13 to be
162 normalized over the volume of the crystal rather than all space, thus ensuring
163 equation 4 is satisfied.

164 The Sommerfeld parameter $s(k)$ describes the enhancement or suppression of
165 charge density in the vicinity of a charge center. Thus $s(k)$ is given by the ratio of
166 the charge density in the presence of the Coulomb center ($Z \neq 0$) to the value in its
167 absence ($Z = 0$). We write

$$168 s(k) = \frac{|\phi_k^Z(0)|^2}{|\phi_k^0(0)|^2} = \mathcal{N}_0\Omega_0 |\phi_k^Z(0)|^2. \quad (14)$$

169 Note that the division by $|\phi_k^0(0)|^2$ implies that the choices of normalization conditions
170 applied in equations 11, 12, and 13 ultimately do not matter, as long as they are
171 applied consistently. Using equation 13, we obtain the result [2, 3]

$$172 s^{3D}(k) = \frac{2\pi Z}{a^*k} \frac{1}{e^{2\pi Z/a^*k} - 1}, \quad (15)$$

173 where we have used the fact that $R_{kl}(0)$ is non-zero only for $l = 0$ and $F(\alpha, \beta, 0) = 1$,
174 and we have restored the definition of ν .

175 For the purposes of trap-assisted recombination, information about the
176 temperature dependence of the Sommerfeld parameter is particularly relevant. At
177 a given temperature, there is a distribution of momenta present in the carriers of
178 the system, which must be averaged over. The temperature-dependent Sommerfeld
179 parameter in 3D, $s^{3D}(T)$, is given by

$$180 s^{3D}(T) = \frac{\int_0^\infty dk k^2 s(k) e^{-\hbar^2 k^2 / 2m^* k_B T}}{\int_0^\infty dk k^2 e^{-\hbar^2 k^2 / 2m^* k_B T}}. \quad (16)$$

181 As will be discussed in Sec. 3, equation 16 may be integrated numerically to obtain
 182 $s^{3D}(T)$ accurately [12]. Alternatively, if we assume that $k \ll 2\pi|Z|/a^*$, $s^{3D}(k)$ may
 183 be approximated as

$$184 \quad s^{3D}(k) \approx \frac{2\pi|Z|}{a^*k} \begin{cases} 1 & Z < 0 \\ e^{-2\pi|Z|/a^*k} & Z > 0 \end{cases} . \quad (17)$$

185 For the attractive interaction, the integration in equation 16 can then be performed
 186 explicitly using equation 17. However, for the repulsive case we must also employ
 187 Laplace's method [34] to approximately evaluate the integral, introducing a second
 188 potential source of error. We can then arrive at an explicit formula for the
 189 temperature-dependent Sommerfeld parameter,

$$190 \quad s^{3D}(T) = \begin{cases} \frac{4}{\sqrt{\pi}} \left[\frac{Z^2 \theta_b}{T} \right]^{1/2} & Z < 0 \\ \frac{8}{\sqrt{3}} \left[\frac{Z^2 \theta_b}{T} \right]^{2/3} \exp \left(-3 \left[\frac{Z^2 \theta_b}{T} \right]^{1/3} \right) & Z > 0 \end{cases} , \quad (18)$$

191 where $\theta_b = m^* e^4 / [32k_B(\epsilon_r \epsilon_0)^2 \hbar^2]$ is a parameter with units of temperature.
 192 (Equation 18 coincides with equation 4.5 of [2].)

193 The range of momenta over which we need to integrate, and hence the validity
 194 of the assumption $k \ll 2\pi|Z|/a^*$, depends on temperature. It is often assumed that
 195 $k \ll 2\pi|Z|/a^*$, and hence equation 18, is valid for all temperatures that are relevant
 196 in the context of recombination, but in Sec. 3 we will explicitly discuss the potential
 197 errors arising from the approximation.

198 2.2. Two Dimensions

199 In 2D, equation 3 is most readily solved in polar coordinates. Once again, separation
 200 of variables permits us to write the envelope function as

$$201 \quad \phi_k^Z(\mathbf{r}) = R_{km}(r) \Theta_m(\theta) , \quad (19)$$

202 where

$$203 \quad \Theta_m(\theta) = \frac{1}{\sqrt{2\pi}} e^{im\theta} . \quad (20)$$

204 The radial function R_{km} satisfies the equation

$$205 \quad \left(\frac{\partial^2}{\partial r^2} + \frac{1}{r} \frac{\partial}{\partial r} - \frac{\gamma}{r} + k^2 - \frac{m^2}{r^2} \right) R_{km}(r) = 0 . \quad (21)$$

206 The solutions to equation 21 take a form similar to equation 7 [35, 36],

$$207 \quad R_{km}(r) = C_{km} e^{-ikr} r^{|m|} F\left(|m| + \frac{1}{2} - i\nu, 2|m| + 1, 2ikr\right) . \quad (22)$$

208 At large distances $r \rightarrow \infty$, the radial equation in 2D takes on the asymptotic form

$$\begin{aligned} R_{km}(r) = & \frac{2C_{km}}{\sqrt{2kr}} \frac{\Gamma(2|m| + 1)}{(2k)^{|m|}} \frac{e^{\pi\nu/2}}{|\Gamma(|m| + \frac{1}{2} + i\nu)|} \times \\ & \cos \left(kr - \nu \log(2kr) - \frac{\pi}{2} \left(|m| + \frac{1}{2} \right) - \sigma_m \right) , \end{aligned} \quad (23)$$

209 where

$$210 \quad \sigma_m = \arg \Gamma(|m| + \frac{1}{2} + i\nu), \quad (24)$$

211 is the complex phase of the Gamma function.

212 In 2D, the normalization condition in k scale is modified to be

$$213 \quad \int_0^\infty dr r R_{km}(r) \int_{k-\Delta k}^{k+\Delta k} dk' R_{k'm}(r) = 1, \quad (25)$$

214 where Δk is a small interval. We thus obtain that

$$215 \quad C_{km} = \sqrt{\frac{k}{\pi}} \frac{(2k)^{|m|}}{\Gamma(2|m|+1)} \sqrt{\frac{2\pi}{1+e^{2\pi\nu}} \prod_{s=0}^{|m|-1} [(s+\frac{1}{2})^2 + \nu^2]}. \quad (26)$$

216 In 2D, the partial-wave basis (chosen to satisfy equation 4) is given by

$$\begin{aligned} \phi_k^Z(\mathbf{r}) &= \frac{1}{\sqrt{\mathcal{N}_0 \Omega_0}} \frac{1}{\sqrt{k}} \times \\ &\quad \sum_{m=0}^{\infty} i^m (2m+1) e^{i\delta_m} P_m(\mathbf{k} \cdot \mathbf{r}/kr) R_{km}(r). \end{aligned} \quad (27)$$

217 R_{km} is the radial wavefunction given in equation 22 with the normalization determined
218 in equation 26. Applying equation 14 with the partial-wave expansion in equation 27
219 gives us the Sommerfeld parameter in 2D,

$$220 \quad s^{2D}(k) = \frac{2}{1 + e^{2\pi Z/a^* k}}, \quad (28)$$

221 This result is remarkably similar to that in 3D (equation 15). Temperature averaging
222 in 2D is performed with

$$223 \quad s^{2D}(T) = \frac{\int_0^\infty dk k s(k) e^{-\hbar^2 k^2 / 2m^* k_B T}}{\int_0^\infty dk k e^{-\hbar^2 k^2 / 2m^* k_B T}}. \quad (29)$$

224 Under the assumption that $k \ll 2\pi|Z|/a^*$, equation 28 may be approximated as

$$225 \quad s^{2D}(k) \approx 2 \begin{cases} 1 & Z < 0 \\ e^{-2\pi|Z|/a^* k} & Z > 0 \end{cases}. \quad (30)$$

226 For the attractive interaction, we immediately obtain the result that the Sommerfeld
227 parameter is (approximately) independent of temperature. Again we apply Laplace's
228 method for the repulsive case. We obtain the explicit formula for the temperature-
229 dependent Sommerfeld parameter in 2D:

$$230 \quad s^{2D}(T) = \begin{cases} 2 & Z < 0 \\ \sqrt{\frac{8\pi}{3}} \left[\frac{8Z^2 \theta_b}{T} \right]^{1/6} \exp\left(-3 \left[\frac{Z^2 \theta_b}{T} \right]^{1/3}\right) & Z > 0 \end{cases}, \quad (31)$$

231 where $\theta_b = m^* e^4 / [32k_B (\epsilon_r \epsilon_0)^2 \hbar^2]$ is a parameter with units of temperature.

232 2.3. One Dimension

233 The Coulomb potential in 1D has long been a subject of research interest—and
 234 controversy [37, 38, 39, 40, 41]. With respect to the definition of the Sommerfeld
 235 parameter, various arguments have shown that the bare Coulomb potential in 1D is
 236 impenetrable [42, 43, 44, 45, 46]. In other words, the wavefunction must be identically
 237 zero at the origin, due to the harsh divergence of the potential. We thus conclude that
 238 the Sommerfeld parameter is identically zero even for an attractive potential in 1D.

239 In some works a modified potential was utilized to soften the divergence [38, 39,
 240 40, 47]; this approach allows us to gain insight into the physical behavior in 1D. The
 241 modification of the bare Coulomb potential is a pragmatic choice since most “one-
 242 dimensional” systems, e.g., nanotubes, are not strictly 1D. While there are several
 243 possible choices for the modified potential, the qualitative conclusions are unaffected
 244 by this choice. Here we will follow the approach of [47].

245 In 1D, there is only one coordinate to account for and no separation of variables
 246 is necessary to solve equation 3. As such, equation 3 is written as

$$247 \left(\frac{d^2}{dx^2} - \frac{\gamma}{|x| + x_0} + k^2 \right) \phi_k^Z(x) = 0, \quad (32)$$

248 where x is the coordinate of interest and $-\infty < x < \infty$ (unlike the radial variable
 249 $0 \leq r < \infty$). x_0 provides a cusp-type cutoff to the Coulomb potential and softens the
 250 divergence. When $x_0 \rightarrow 0$, the bare Coulomb potential is obtained.

251 Equation 32 can be written in the form of the Whittaker equation [48, 32, 33] by a
 252 suitable change of variables $z = 2ik(|x| + x_0)$. We introduce ν' , defined as $\nu' = |Z|/a^*k$,
 253 and first focus on the attractive case ($Z < 0$). With this transformation, we obtain

$$254 \left(\frac{d^2}{dz^2} + \frac{i\nu'}{z} - \frac{1}{4} \right) \phi_k^Z(x) = 0, \quad (33)$$

255 which is the special case of the Whittaker equation where $\mu = 1/2$ in equation 9.220.1
 256 of [32]. For the repulsive case, we take $\nu' \rightarrow -\nu'$; we are then free to take $z \rightarrow -z$,
 257 leaving equation 33 unchanged. We thus find that the repulsive and attractive
 258 Sommerfeld parameter in 1D are identical.

259 Equation 33 has four possible solutions $W_{\pm i\nu}(\pm z)$, which are linear combinations
 260 of the regular and irregular confluent hypergeometric series. The regular confluent
 261 hypergeometric series (equation 8) was used in the derivation for both 2D and 3D; in
 262 1D, the irregular series is also a valid solution. The explicit form of $W_{\pm i\nu}(\pm z)$ is given
 263 by equation 9.220.4 in [32].

264 The physically relevant solution to equation 33 is given by

$$265 \phi_k^Z(x) = AW_{-i\nu}(z) + BW_{i\nu}(-z), \quad (34)$$

266 where A and B are normalization coefficients to be determined. Based on the physics,
 267 we know that the solution, which is non-zero at the origin for finite x_0 , should be an
 268 even function and obey

$$269 \frac{d}{dz} \phi_k^Z(x)|_{x=0} = 0. \quad (35)$$

270 Introducing $D_0 = \frac{d}{dz} W_{-i\nu}(z)|_{x=0}$ and $D_1 = \frac{d}{dz} W_{i\nu}(-z)|_{x=0}$, we can apply equation 35
 271 to write the envelope function (equation 34) as

$$272 \phi_k^Z(x) = N [D_1 W_{-i\nu}(z) - D_0 W_{i\nu}(-z)], \quad (36)$$

273 where $N = A/D_1$ is a normalization coefficient to be determined.

274 The asymptotic form of $W_{i\nu}(z)$ as $z \rightarrow \infty$ is

$$275 \quad W_{i\nu}(z) \sim e^{-z/2} z^{i\nu} . \quad (37)$$

276 In 1D, we apply the normalization condition

$$277 \quad \int_{-\infty}^{\infty} dx \phi_k^Z(x) \int_{k-\Delta k}^{k+\Delta k} dk' \phi_{k'}^Z(x) = \frac{\pi}{\mathcal{N}_0 \Omega_0} . \quad (38)$$

278 (The chosen normalization condition enforces equation 4 and differs from
279 normalization in higher dimensions since the partial-wave basis is not invoked.) We
280 obtain

$$281 \quad N = \sqrt{\frac{e^{-\pi\nu}}{2\mathcal{N}_0\Omega_0}} (|D_0|^2 + |D_1|^2)^{-1/2} . \quad (39)$$

282 Applying equation 14 gives us the Sommerfeld parameter in 1D

$$283 \quad s^{1D}(k) = \frac{e^{-\pi\nu}}{2} \frac{|D_1 W_{-i\nu}(z_0) - D_0 W_{i\nu}(-z_0)|^2}{|D_0|^2 + |D_1|^2} , \quad (40)$$

284 where $z_0 = 2ikx_0$. Given the complexity of this expression, we do not attempt
285 to obtain an analytical form for the temperature dependence of the Sommerfeld
286 parameter in 1D. The temperature-dependent Sommerfeld parameter in 1D can be
287 obtained by numerically integrating

$$288 \quad s^{1D}(T) = \frac{\int_0^{\infty} dk s(k) e^{-\hbar^2 k^2 / 2m^* k_B T}}{\int_0^{\infty} dk e^{-\hbar^2 k^2 / 2m^* k_B T}} . \quad (41)$$

289 3. Discussion

290 The Sommerfeld parameter as a function of momentum is shown in figure 1. Focusing
291 first on the repulsive Sommerfeld parameter [figure 1(a)], we find that independent of
292 dimensionality the Sommerfeld parameter is less than one, which leads to a suppression
293 of trap-assisted recombination. In all cases, $s(k \rightarrow \infty) = 1$ as expected. We find that
294 the functions in 3D and 2D have a similar qualitative structure, with 2D leading to a
295 stronger suppression. In 1D, the divergence of the Coulomb potential was suppressed
296 with a cusp-type cutoff set by the parameter x_0 . We see that as x_0 approaches zero,
297 $s(k)$ also approaches zero for all k , confirming that the bare Coulomb potential in
298 1D is impenetrable. However, in order for $s(k)$ to truly approach zero, exceedingly
299 small values of x_0 are required; we see that $s(k)$ still has significant nonzero values
300 even if x_0 is as small as $10^{-8}a^*$, illustrating that true one-dimensional systems, for
301 which $s(k) = 0$ should be rigorously zero for all k , are essentially unattainable. For
302 $x_0 = 10^{-3}a^*$, we find that $s(k)$ has a similar magnitude as in 2D and 3D; however,
303 the behavior at small k is distinctly different for 1D, and we will see that this impacts
304 the temperature dependence.

305 The attractive Sommerfeld parameter [figure 1(b)] leads to an enhancement of
306 recombination in 2D and 3D. In contrast, in 1D, the Sommerfeld parameter is still
307 suppressive. We see that the divergence at small k in 3D is softened into a plateau in
308 2D. Again in all cases, $s(k \rightarrow \infty) = 1$ as expected.

309 In the context of trap-assisted recombination, the temperature-dependent
310 Sommerfeld parameter is more relevant. The numerically integrated Sommerfeld
311 parameter is shown in figure 2 for realistic materials parameters ($m^* = 0.1$ and
312 $\epsilon_r = 10$) as a function of temperature. We see that the qualitative conclusions from

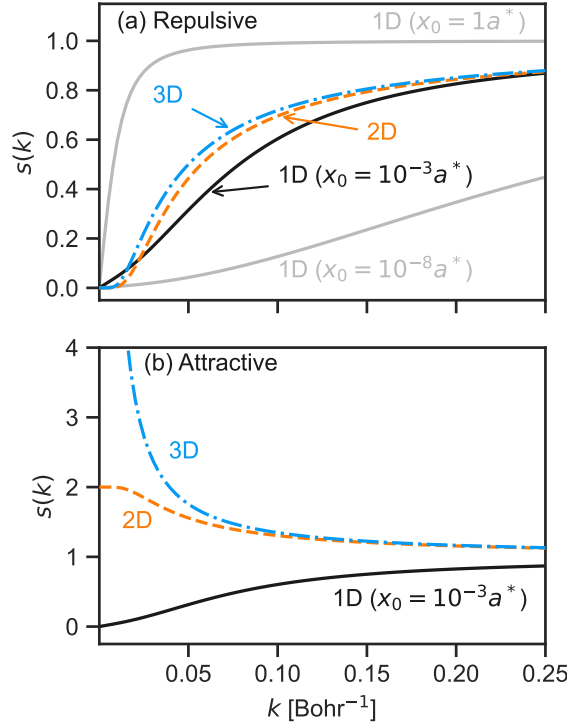


Figure 1. (a) Repulsive and (b) attractive Sommerfeld parameter for $m^* = 0.1$ and $\epsilon_r = 10$ as a function of momentum k . The blue dashed-dotted line corresponds to 3D. The orange dashed line corresponds to 2D. The grey solid lines and the black line correspond to different choices of the cutoff parameter x_0 in 1D.

313 the analysis of the momentum dependence hold true. For the repulsive interaction
 314 [figure 2(a)], a suppression is observed across all temperatures. The low-temperature
 315 behavior in 1D differs from the 2D and 3D cases. The true-1D case would give
 316 $s(T) = 0$; finite values occur only because of the introduction of a cusp-type cutoff
 317 to the Coulomb potential. Smaller x_0 values lead to lower values of $s(T)$. For a given x_0 ,
 318 the suppression of these finite values at low T is less pronounced in 1D than in 2D or
 319 3D. While the exact numerical values depend on the choice of the modified potential,
 320 these qualitative conclusions are unaffected.

321 For the attractive interaction [figure 2(b)], the effects of dimensionality are
 322 more pronounced. We see that in 3D, a divergent enhancement is obtained at low
 323 temperatures. In 2D, the Sommerfeld parameter leads to an enhancement ($s = 2$) but
 324 is effectively independent of temperature. In 1D, even an attractive potential leads
 325 to a suppression ($s < 1$), and $s(T)$ decreases at low temperature.

326 In 3D and 2D, an analytical form for the temperature-dependent Sommerfeld
 327 parameter (Eqs. 16 and 29, respectively) was obtained. However, the derivation
 328 relied on approximations to simplify the expressions: it has been shown that these
 329 approximations may not be strictly valid over the range of temperatures where they
 330 are employed [12]. The relative error of the analytical expressions compared to direct

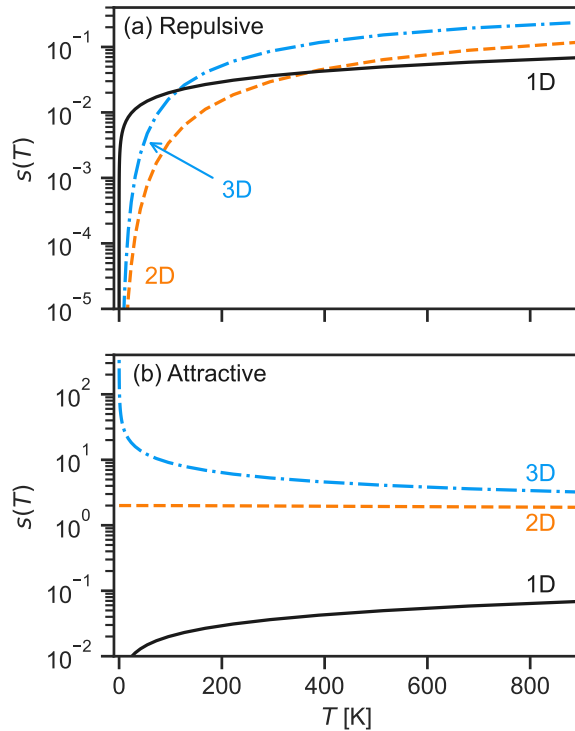


Figure 2. (a) Repulsive and (b) attractive Sommerfeld parameter for $m^* = 0.1$ and $\epsilon_r = 10$ as a function of temperature T . The blue dashed-dotted line corresponds to 3D. The orange dashed line corresponds to 2D. The black solid line corresponds to 1D with $x_0 = 10^{-3}a^*$.

331 numerical evaluation is shown in figure 3. We find that the error is comparable for
 332 the attractive interaction in 3D and 2D. The error is most severe for the repulsive
 333 interaction in 3D. For the repulsive interaction in 2D, a fortuitous cancellation between
 334 the assumption that k is small ($k \ll 2\pi|Z|/a^*$) and the use of Laplace's method
 335 leads to a marked decrease in the relative error. Still, since most applications of
 336 the Sommerfeld parameter rely on numerical results, there is no particular need to
 337 use the approximation and we recommend utilizing the numerical evaluation of the
 338 temperature dependence to avoid spurious errors.

339 In our derivation, we assumed an isotropic, non-degenerate band extremum at
 340 the Γ point. These assumptions do not affect the generality of our results. When
 341 anisotropy is present, we recommend choosing an appropriately averaged effective
 342 mass with the derived equations to account for this effect. In materials where the
 343 band extremum does not occur at the Γ point, there will be a valley degeneracy
 344 that needs to be accounted for. Furthermore, there may be orbital degeneracy. In
 345 most cases, degeneracy can simply be handled by including a multiplicative factor and
 346 retaining the same functional form of the Sommerfeld parameter derived here. We have
 347 implicitly assumed that screening effects are negligible and do not lead to substantial
 348 deviations from the ideal $1/r$ behavior at large distances [2]. This assumption is

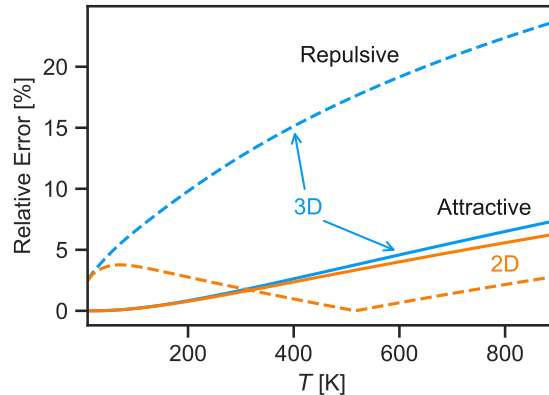


Figure 3. Relative error of the analytical expression (Eqs. 18 and 31) compared to direct numerical evaluation (Eqs. 16 and 29) of the temperature-dependent Sommerfeld parameter. The blue lines correspond to 3D, and orange lines correspond to 2D. Solid lines are for the attractive interaction, dashed lines for the repulsive interaction. Here we utilize $m^* = 0.1$ and $\epsilon_r = 10$.

349 consistent with low to modest carrier densities. Furthermore, this means that we do
 350 not attempt to address 2D electron or hole gases, which have much higher carrier
 351 densities. We also assume dilute defect concentrations, for which the overlap of the
 352 Coulomb potential can be neglected.

353 The developments detailed here have now been added to the Nonrad code [25, 12]
 354 in version 1.2. When treating trap-assisted recombination in lower dimensions, there
 355 may be effects beyond just the Sommerfeld parameter, such as quantum confinement,
 356 strain, or nonidealities at the surface or interface. These are best handled within the
 357 recombination rate evaluation (e.g., by changing the input parameters that enter the
 358 Nonrad code).

359 4. Implications

360 Our results clearly show that decreased dimensionality suppresses trap-assisted
 361 recombination. The effect is most clear in the attractive interaction: While both
 362 3D and 2D result in an enhancement, the enhancement in 2D can be far less than that
 363 of 3D and is independent of temperature. For example, the Sommerfeld parameter
 364 takes a value of 44.5 at 4 K and 5.2 at 300 K in 3D when $\epsilon_r = 10$ and $m^* = 0.1$. This is
 365 compared to a value of 2 for 2D, independent of temperature. In 1D, an enhancement
 366 is no longer possible, only a suppression; we obtain a value of 0.004 at 4 K and 0.04
 367 at 300 K for the same ϵ_r and m^* when $x_0 = 10^{-3}a^*$.

368 The Sommerfeld parameters do not strongly depend on ϵ_r and m^* , for values of
 369 these parameters that are typical for semiconductors and insulators. The Sommerfeld
 370 parameter becomes less important [i.e., $s(T)$ approaches 1] as $\epsilon_r \rightarrow \infty$ or $m^* \rightarrow 0$.
 371 Indeed, larger values of ϵ_r correspond to increased screening of the potential, and for
 372 smaller values of m^* , the particle moves faster at a given temperature and is less
 373 subject to the effects of the potential.

374 These results have important implications for the physics of real materials and

375 their applications. Optoelectronic devices commonly employ quantum-well structures,
376 layers of material that can be as thin as a few unit cells, sandwiched between layers
377 of a material with a larger band gap, effectively confining the carriers in the quantum
378 well. The trend to reduce device dimensions in electronics also leads to situations
379 where carriers behave as if confined in 2D or 1D. Our results indicate that the
380 decreasing the dimensionality leads to a reduction in trap-assisted recombination.
381 Notably, the temperature dependence in 3D and 2D is different: experiments that
382 probe low-temperature trap-assisted recombination rates should be able to discern
383 whether dimensionality is playing a role.

384 Another area in which the dimensionality clearly plays a role is in two-dimensional
385 materials, which are candidates for electronic device applications thanks in part to
386 the ability to construct van der Waals heterostructures [18]. Our results point out
387 an additional benefit of such devices: trap-assisted recombination will be suppressed
388 compared to their bulk counterparts. Two-dimensional materials are also promising
389 as hosts for quantum defects [19, 20, 21, 49, 50, 51, 52]; for example, a single
390 defect embedded in a monolayer of material can be used as a quantum sensor with
391 superior resolution. Carrier trapping at a defect can ruin its quantum properties; the
392 suppression provided by the Sommerfeld parameter could mitigate this process in a
393 2D material. Going further, even one-dimensional materials, such as nanotubes, are
394 being considered as hosts for quantum defects [23, 24]; they would further benefit from
395 the suppression provided by the Sommerfeld parameter.

396 5. Conclusions

397 In conclusion, we have examined the effect of dimensionality on trap-assisted
398 recombination through the Sommerfeld parameter. We derived the temperature-
399 dependent Sommerfeld parameter in 2D and 1D, and obtained an approximate
400 analytical expression in 2D. In 1D, the bare Coulomb potential leads to an identically
401 zero Sommerfeld parameter; a more realistic description was presented by introducing
402 a cusp-type cutoff of the potential. Overall we find that a lowering of dimensionality
403 reduces trap-assisted recombination. This effect is most obvious for an attractive
404 interaction: in 3D, the Sommerfeld parameter leads to an enhancement of trap-assisted
405 recombination; this enhancement is reduced in 2D, while in 1D, a suppression occurs
406 (even when using the cutoff of the Coulomb potential). The formulas derived in this
407 work have now been implemented in the latest version of the Nonrad code [25, 12].

408 Acknowledgments

409 We dedicate this work to the memory of Audrius Alkauskas, an outstanding scientist,
410 generous colleague, and caring friend. This work was supported by the U.S.
411 Department of Energy, Office of Science, National Quantum Information Science
412 Research Centers, Co-design Center for Quantum Advantage (C2QA) under contract
413 number DE-SC0012704. The research used resources of the National Energy Research
414 Scientific Computing Center, a DOE Office of Science User Facility supported by the
415 Office of Science of the U.S. Department of Energy under Contract No. DE-AC02-
416 05CH11231 under NERSC award BES-ERCAP0021021.

417 [1] Sommerfeld A 1931 *Annalen der Physik* **403** 257–330 ISSN 1521-3889

418 [2] Pässler R 1976 *Phys. Status Solidi B* **78** 625–635 ISSN 03701972, 15213951

- 419 [3] Landsberg P T 2003 *Recombination in Semiconductors* 1st ed (Cambridge: Cambridge
420 University Press) ISBN 978-0-521-54343-9
- 421 [4] Abakumov V N, Perel V I and Yassievich I N 1991 *Nonradiative Recombination in*
422 *Semiconductors (Modern Problems in Condensed Matter Sciences no 33)* (Amsterdam:
423 North-Holland) ISBN 978-0-444-88854-9
- 424 [5] Landau L D, Lifšic E M and Landau L D 2007 *Quantum Mechanics: Non-Relativistic Theory*
425 3rd ed (*Course of Theoretical Physics / by L. D. Landau and E. M. Lifshitz no 3*) (Singapore:
426 Elsevier) ISBN 978-0-7506-3539-4 978-981-272-088-7 978-7-5062-4257-8
- 427 [6] Arkani-Hamed N, Finkbeiner D P, Slatyer T R and Weiner N 2009 *Phys. Rev. D* **79** 015014
- 428 [7] Blum K, Sato R and Slatyer T R 2016 *J. Cosmol. Astropart. Phys.* **2016** 021–021 ISSN 1475-
429 7516
- 430 [8] Iengo R 2009 *J. High Energy Phys.* **2009** 024–024 ISSN 1029-8479
- 431 [9] Alkauskas A, Yan Q and Van de Walle C G 2014 *Phys. Rev. B* **90** 075202
- 432 [10] Shi L, Xu K and Wang L W 2015 *Phys. Rev. B* **91** 205315 ISSN 1098-0121, 1550-235X
- 433 [11] Wickramaratne D, Shen J X, Alkauskas A and Van de Walle C G 2018 *Phys. Rev. B* **97** ISSN
434 2469-9950, 2469-9969
- 435 [12] Turiansky M E, Alkauskas A, Engel M, Kresse G, Wickramaratne D, Shen J X, Dreyer C E and
436 Van de Walle C G 2021 *Comput. Phys. Commun.* **267** 108056 ISSN 00104655
- 437 [13] Dreyer C E, Alkauskas A, Lyons J L and Van de Walle C G 2020 *Phys. Rev. B* **102** 085305
- 438 [14] Zhao F, Turiansky M E, Alkauskas A and Van de Walle C G 2023 *Phys. Rev. Lett.* **131** 056402
439 ISSN 0031-9007, 1079-7114
- 440 [15] Goktas N I, Wilson P, Ghukasyan A, Wagner D, McNamee S and LaPierre R R 2018 *Appl. Phys.*
441 *Rev.* **5** 041305 ISSN 1931-9401
- 442 [16] Zhang B, Li Z, Wu H, Pendharkar M, Dempsey C, Lee J S, Harrington S D, Palmstrom C J
443 and Frolov S M 2023 Supercurrent through a single transverse mode in nanowire Josephson
444 junctions (*Preprint* **2306.00146**)
- 445 [17] Aghaee M, Akkala A, Alam Z, Ali R, Alcaraz Ramirez A, Andrzejczuk M, Antipov A E, Aseev
446 P, Astafev M, Bauer B, Becker J, Boddapati S, Boekhout F, Bommer J, Bosma T, Bourdet L,
447 Boutin S, Caroff P, Casparis L, Cassidy M, Chatoor S, Christensen A W, Clay N, Cole W S,
448 Corsetti F, Cui A, Dalampiras P, Dokania A, De Lange G, De Moor M, Estrada Saldaña
449 J C, Fallahi S, Fathabad Z H, Gamble J, Gardner G, Govender D, Griggio F, Grigoryan
450 R, Gronin S, Gukelberger J, Hansen E B, Heedt S, Herranz Zamorano J, Ho S, Holgaard
451 U L, Ingerslev H, Johansson L, Jones J, Kallaher R, Karimi F, Karzig T, King C, Kloster
452 M E, Knapp C, Kocon D, Koski J, Kostamo P, Krogstrup P, Kumar M, Laeven T, Larsen
453 T, Li K, Lindemann T, Love J, Lutchyn R, Madsen M H, Manfra M, Markussen S, Martinez
454 E, McNeil R, Memisevic E, Morgan T, Mullally A, Nayak C, Nielsen J, Nielsen W H P,
455 Nijholt B, Nurmohamed A, O'Farrell E, Otani K, Pauka S, Petersson K, Petit L, Pikulin
456 D I, Preiss F, Quintero-Perez M, Rajpalke M, Rasmussen K, Razmadze D, Reentila O, Reilly
457 D, Rouse R, Sadvovskyy I, Sainiemi L, Schreppler S, Sidorkin V, Singh A, Singh S, Sinha
458 S, Sohr P, Stankevič T, Stek L, Suominen H, Suter J, Svidenko V, Teicher S, Temuerhan
459 M, Thiyagarajah N, Tholapi R, Thomas M, Toomey E, Upadhyay S, Urban I, Vaitiekėnas
460 S, Van Hoogdalem K, Van Woerkom D, Viazmitinov D V, Vogel D, Waddy S, Watson J,
461 Weston J, Winkler G W, Yang C K, Yau S, Yi D, Yucelen E, Webster A, Zeisel R, Zhao R
462 and Microsoft Quantum 2023 *Phys. Rev. B* **107** 245423 ISSN 2469-9950, 2469-9969
- 463 [18] Geim A K and Grigorieva I V 2013 *Nature* **499** 419–425 ISSN 1476-4687
- 464 [19] Kubanek A 2022 *arXiv:2201.13184*
- 465 [20] Turiansky M E, Alkauskas A and Van de Walle C G 2020 *Nat. Mater.* **19** 487–489 ISSN 1476-
466 4660
- 467 [21] Turiansky M E, Alkauskas A, Bassett L C and Van de Walle C G 2019 *Phys. Rev. Lett.* **123**
468 127401
- 469 [22] Gottscholl A, Diez M, Soltamov V, Kasper C, Krauße D, Sperlich A, Kianinia M, Bradac C,
470 Aharonovich I and Dyakonov V 2021 *Nat. Commun.* **12** 4480 ISSN 2041-1723
- 471 [23] Ma X, Hartmann N F, Baldwin J K S, Doorn S K and Htoon H 2015 *Nat. Nanotechnol.* **10**
472 671–675 ISSN 1748-3395
- 473 [24] Ahn J, Xu Z, Bang J, Allcca A E L, Chen Y P and Li T 2018 *Opt. Lett.* **43** 3778 ISSN 0146-9592,
474 1539-4794
- 475 [25] Turiansky M E, Shen J X, Alkauskas A and Van de Walle C G 2023 Nonrad URL <https://doi.org/10.5281/zenodo.4274317>
476
- 477 [26] Luttinger J M and Kohn W 1955 *Phys. Rev.* **97** 869–883 ISSN 0031-899X
- 478 [27] Wannier G H 1937 *Phys. Rev.* **52** 191–197 ISSN 0031-899X
- 479 [28] Kohn W and Luttinger J M 1955 *Phys. Rev.* **97** 883–888 ISSN 0031-899X

- 480 [29] Slater J C 1949 *Phys. Rev.* **76** 1592–1601 ISSN 0031-899X
- 481 [30] Luttinger J M 1951 *Phys. Rev.* **84** 814–817 ISSN 0031-899X
- 482 [31] Bethe H A and Salpeter E E 1977 *Quantum Mechanics of One- and Two-Electron Atoms*
483 (Boston, MA: Springer US) ISBN 978-1-4613-4104-8
- 484 [32] Gradshteyn I S and Ryzhik I M 2015 *Table of Integrals, Series, and Products* (Kent: Elsevier
485 Science) ISBN 978-1-4832-6564-3
- 486 [33] *NIST Digital Library of Mathematical Functions* <http://dlmf.nist.gov/>, Release 1.1.7 of 2022-
487 10-15 F. W. J. Olver, A. B. Olde Daalhuis, D. W. Lozier, B. I. Schneider, R. F. Boisvert,
488 C. W. Clark, B. R. Miller, B. V. Saunders, H. S. Cohl, and M. A. McClain, eds. URL
489 <http://dlmf.nist.gov/>
- 490 [34] Butler R W 2007 *Saddlepoint Approximations with Applications* Cambridge Series in Statistical
491 and Probabilistic Mathematics (Cambridge: Cambridge University Press) ISBN 978-0-521-
492 87250-8
- 493 [35] Yang X L, Guo S H, Chan F T, Wong K W and Ching W Y 1991 *Phys. Rev. A* **43** 1186–1196
494 ISSN 1050-2947, 1094-1622
- 495 [36] Yang X L 1990 *Analytic Solution of a Two-Dimensional Hydrogen Atom* Ph.D. thesis University
496 of Arkansas
- 497 [37] Downing C A and Portnoi M E 2014 *Phys. Rev. A* **90** 052116 ISSN 1050-2947, 1094-1622
- 498 [38] Haines L K and Roberts D H 1969 *Am. J. Phys.* **37** 1145–1154 ISSN 0002-9505
- 499 [39] Loudon R 1959 *Am. J. Phys.* **27** 649–655 ISSN 0002-9505
- 500 [40] Loudon R 2016 *Proc. Math. Phys. Eng. Sci.* **472** 20150534 ISSN 1364-5021, 1471-2946
- 501 [41] Moshinsky M 1993 *J. Phys. A Math. Gen.* **26** 2445–2450 ISSN 0305-4470, 1361-6447
- 502 [42] Abramovici G and Avishai Y 2009 *J. Phys. A Math. Theor.* **42** 285302 ISSN 1751-8113, 1751-
503 8121
- 504 [43] Andrews M 1976 *Am. J. Phys.* **44** 1064–1066 ISSN 0002-9505, 1943-2909
- 505 [44] Gomes J F and Zimmerman A H 1980 *Am. J. Phys.* **48** 579–580 ISSN 0002-9505, 1943-2909
- 506 [45] Newton R G 1994 *J. Phys. A Math. Gen.* **27** 4717–4718 ISSN 0305-4470, 1361-6447
- 507 [46] Núñez-Yépez H N, Salas-Brito A L and Solis D A 2011 *Phys. Rev. A* **83** 064101 ISSN 1050-2947,
508 1094-1622
- 509 [47] Ogawa T and Takagahara T 1991 *Phys. Rev. B* **44** 8138–8156 ISSN 0163-1829, 1095-3795
- 510 [48] Whittaker E T 1903 *Bull. Am. Math. Soc.* **10** 125–134 ISSN 0273-0979, 1088-9485
- 511 [49] Turiansky M E and Van de Walle C G 2021 *J. Appl. Phys.* **129** 064301 ISSN 0021-8979
- 512 [50] Parto K, Azzam S I, Banerjee K and Moody G 2021 *Nat. Commun.* **12** 3585 ISSN 2041-1723
- 513 [51] Luo Y, Shepard G D, Ardelean J V, Rhodes D A, Kim B, Barmak K, Hone J C and Strauf S
514 2018 *Nat. Nanotechnol.* **13** 1137–1142 ISSN 1748-3387, 1748-3395
- 515 [52] Lee Y, Hu Y, Lang X, Kim D, Li K, Ping Y, Fu K M C and Cho K 2022 *Nat. Commun.* **13**
516 7501 ISSN 2041-1723